

Thermal Analysis of Iodine Satellite (iSAT)

Stephanie Mauro¹

NASA Marshall Space Flight Center, Huntsville AL 35812

This paper presents the progress of the thermal analysis and design of the Iodine Satellite (iSAT). The purpose of the iSAT spacecraft (SC) is to demonstrate the ability of the iodine Hall Thruster propulsion system throughout a one year mission in an effort to mature the system for use on future satellites. The benefit of this propulsion system is that it uses a propellant, iodine, that is easy to store and provides a high thrust-to-mass ratio. The spacecraft will also act as a bus for an earth observation payload, the Long Wave Infrared (LWIR) Camera. Four phases of the mission, determined to either be critical to achieving requirements or phases of thermal concern, are modeled. The phases are the Right Ascension of the Ascending Node (RAAN) Change, Altitude Reduction, De-Orbit, and Science Phases. Each phase was modeled in a worst case hot environment and the coldest phase, the Science Phase, was also modeled in a worst case cold environment. The thermal environments of the spacecraft are especially important to model because iSAT has a very high power density. The satellite is the size of a 12 unit cubesat, and dissipates slightly more than 75 Watts of power as heat at times. The maximum temperatures for several components are above their maximum operational limit for one or more cases. The analysis done for the first Design and Analysis Cycle (DAC1) showed that many components were above or within 5°C of their maximum operation limit. The battery is a component of concern because although it is not over its operational temperature limit, efficiency greatly decreases if it operates at the currently predicted temperatures. In the second Design and Analysis Cycle (DAC2), many steps were taken to mitigate the overheating of components, including isolating several high temperature components, removal of components, and rearrangement of systems. These changes have greatly increased the thermal margin available.

Nomenclature

<i>Al</i>	=	Aluminum
<i>BOL</i>	=	Beginning of Life
<i>°C</i>	=	Degrees Celcius
<i>CAD</i>	=	Computer Aided Design
<i>C&DH</i>	=	Command and Data Handling
<i>DAC</i>	=	Design and Analysis Cycle
<i>EIB</i>	=	Extra Interfaces Board
<i>EOL</i>	=	End of Life
<i>FC</i>	=	Flight Computer
<i>FL</i>	=	Fuel Lines
<i>FLUINT</i>	=	Fluid Integrator
<i>GN&C</i>	=	Guidance, Navigation, and Control
<i>GPS</i>	=	Global Positioning System
<i>IMU</i>	=	Inertial Measurement Unit
<i>in</i>	=	inches
<i>IR</i>	=	Infrared
<i>iSAT</i>	=	Iodine Satellite
<i>kg</i>	=	kilogram
<i>LVLH</i>	=	Local Vertical Local Horizon

¹ Thermal Engineer, MSFC ES22: Space Systems Department, Thermal and Mechanical Analysis Branch

<i>LWIR</i>	=	Long Wavelength Infrared
<i>m</i>	=	Meter
<i>MIL</i>	=	Military Standard
<i>min</i>	=	minute
<i>MLI</i>	=	Multilayer Insulation
<i>mm</i>	=	millimeter
<i>MT</i>	=	Magnetorquer
<i>MW</i>	=	Momentum Wheels
<i>OSR</i>	=	Optical Solar Radiator
<i>PCB</i>	=	Printed Circuit Board
<i>PDB</i>	=	Power Distribution List
<i>PDR</i>	=	Preliminary Design Review
<i>PFCV</i>	=	Proportional Flow Control Valve
<i>PMB</i>	=	Power Management Board
<i>PPU</i>	=	Power Processing Unit
<i>PT</i>	=	Pressure Transducer
<i>RAAN</i>	=	Right Ascension of the Ascending Node
<i>RADk</i>	=	Radiation Conductor
<i>s</i>	=	second
<i>SC</i>	=	Spacecraft
<i>SINDA</i>	=	Systems Improved Numerical Differencing Analyzer
<i>SS</i>	=	Sun Sensor
<i>ST</i>	=	Star Tracker
<i>TD</i>	=	Thermal Desktop
<i>Temp</i>	=	Temperature
<i>U</i>	=	Unit
<i>W</i>	=	Watt

I. Introduction

The iSAT models discussed in this paper include models from both DAC1 and DAC2. The DAC1 model is created based on the spacecraft configuration and assumptions used for the Preliminary Design Review (PDR). The DAC2 model is built from the configuration created following PDR, as a result of comments made during the review and issues which arose from the needed changes. The DAC2 updates were made in the five months following PDR.

Four phases of the iSAT mission are modeled for DAC1 analysis: the Right Ascension of the Ascending Node (RAAN) Change, Altitude Reduction, De-Orbit, and Science Phases. Each of these phases completes a task necessary to fulfilling requirements throughout the year long mission of the spacecraft. The RAAN Change Phase will use the iodine Hall Thruster propulsion system to change the orbit inclination, the Altitude Reduction phase will fire the thruster to lower the spacecraft to the science orbit, the De-Orbit Phase will perform a maneuver to ensure that the spacecraft enters the earth's atmosphere within the specified period of time, and the Science Phase will operate the payload. The Science Phase is the only phase modeled in which the thruster is not fired. In the thermal model, there are two differences between each phase which are adjusted based on the operation timeline. The first is the heat dissipation with respect to time of each component. The second is the orientation of the spacecraft throughout the orbit. A worst case hot analysis was performed for each phase, and a worst case cold analysis was also performed for the Science Phase, the coldest phase modeled. Because the orbit details and exact altitude remain unknown, the Hot Case assumes the hottest possible environment with the SC at the lowest possible altitude and the highest possible beta angle, resulting in the greatest albedo heating from the earth, and a Dawn-Dusk orbit, in which the SC is always in view of the sun. The Cold Case assumes the coldest possible environment with the SC at the highest possible altitude and the lowest possible beta angle, resulting in the least amount of albedo heating from the earth, and a Noon-Midnight orbit, in which the SC is in the earth's eclipse for 37% of the orbit.

Included in the model are all powered components, the chassis, and solar panel assemblies. Most secondary fixtures are not explicitly modeled. The only component mounts modeled are the camera and cathode mounts. The mounting interfaces for inner components and hinges between the chassis and solar panel mountplates are simplified

as contactors with no geometry modeled to represent the mass. Component dimensions and locations were measured from the Mechanical Design Computer Aided Design (CAD) model and built in the thermal model. Figure 1 shows the CAD and Thermal Desktop (TD) model of the entire satellite for the first Design and Analysis Cycle (DAC1). Components within the enclosure are not visible from the view. The thruster shown is the iodine Hall Effect Thruster, which is comprised of an anode and a cathode. The anode is included in the cylindrical housing, simplified in the TD model, and the cathode is modeled as its own component.

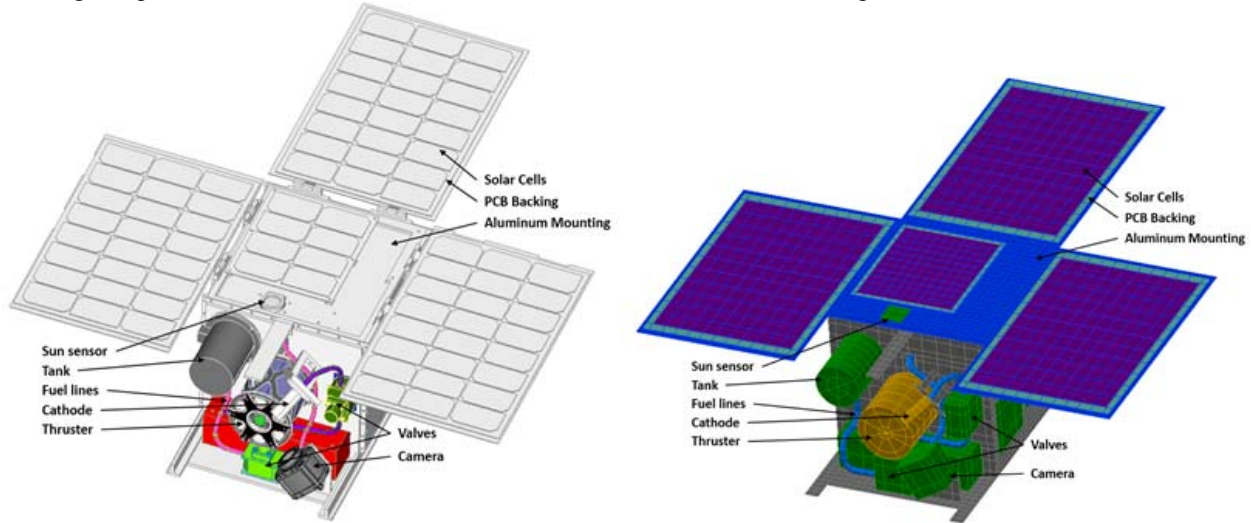


Figure 1. CAD Model (left) and Thermal Model (right) of iSAT

Figure 2 shows a view of the model revealing the inside the enclosure. Hidden components include the Aluminum Solar Panel Mounting, Printed Circuit Board (PCB) Solar Panel Backing, Solar Cells, two of the enclosure faces, and all of the components outside of the enclosure. In the thermal model the components along the walls are attached via a thermal contact, not a physical mount geometry, as in the CAD model.

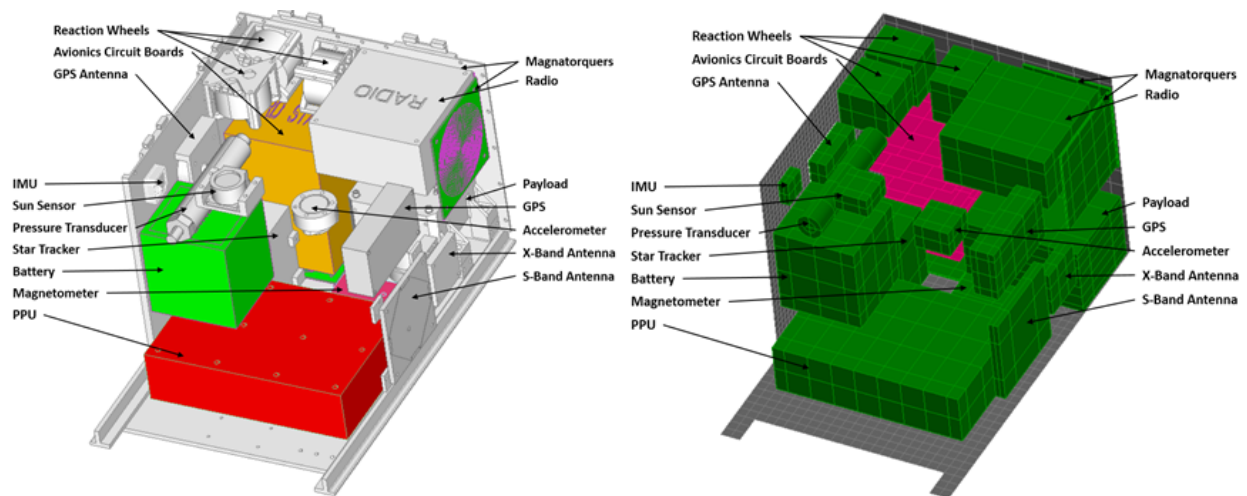


Figure 2. CAD Model (left) and Thermal Model (right) of iSAT Components Within Chassis

The card stack detail is shown in Figure 3. In the CAD model, a card stack envelope is modeled to ensure that the space for the card stack is reserved, but in the thermal model, the cards are each modeled individually, with no housing. Like the components, each card is attached to the enclosure via a thermal contact.

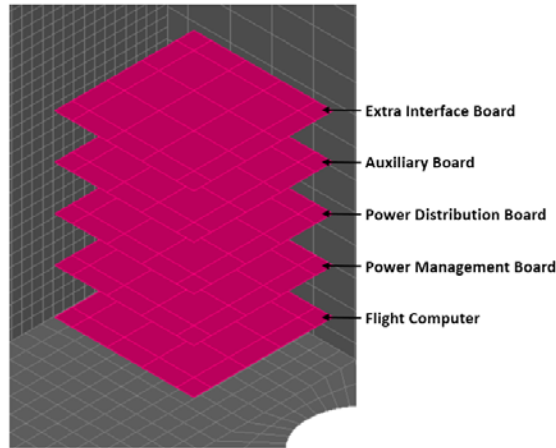


Figure 3. Thermal Model Cards Stack Detail

Additional views of the components within the spacecraft are included in Appendix A.

II. Model Details

The thermal model was built in Thermal Desktop¹ (TD) and analyzed with SINDA/FLUINT².

A. Components

The thermal analysis model of iSAT was built to perform analyses to assess component temperatures throughout the key phases of the mission. The components individually modeled are:

- Power
 - Power Management Board (PMB)
 - Power Distribution Board (PDB)
 - Lithium-Polymer Battery
 - Solar Cells
- Guidance, Navigation and Control (GN&C)
 - Reaction Wheels
 - Star Tracker
 - Inertial Measurement Unit (IMU)
 - Magnetic Torquers (MT)
 - Global Positioning System (GPS) Receiver
 - GPS Antenna
- Communications
 - Radio
 - 3 circuit boards
 - enclosure
 - S-Band Antenna
 - X-Band Antenna
- Command and Data Handling (C&DH)
 - Flight Computer (FC)
 - Auxiliary Board (AB)
 - Extra Interfaces Board (EIB)
- Propulsion:
 - Thruster
 - Anode
 - Cathode
 - Thruster Camera
 - 2 Proportional Flow Control Valves (PFCV)
 - PFCV Heaters
 - Power Processing Unit (PPU)
 - Fuel (in fuel tank)
 - Fuel Tank
 - Fuel Tank Heater
 - Fuel Lines (FL)
 - FL Heaters
 - Pressure Transducer (PT)
 - PT Heater
- Payload
 - Long Wave Infrared (LWIR) Camera
- Structure
 - Chassis
 - Chassis Outside Radiators
 - Solar Panel Mountplate
 - Optical Solar Radiators (OSR)
 - Solar Panel Printed Circuit Board (PCB) Backing
 - Cathode Mount
 - Thruster Camera Mount

The avionics circuit boards (power management, power distribution, auxiliary, extra interface and the flight computer) were each modeled separately as a surface. The Radio was modeled as three circuit boards with an enclosure built surrounding the boards. The Tank was modeled as a cylindrical shell surface with two circle-shaped surfaces as the top and bottom, creating a closed, hollow cylinder. All other components were built as a solid brick with a pre-designated bulk material and outside coating. Each component has a density multiplier applied to represent the correct mass. Furthermore, the OSR is not explicitly modeled, but is a coating applied to the side on the Solar Panel Mountplates to which the Solar Panel PCB Backing is not mounted. This is also true for the chassis radiators, which are created by covering all outside chassis surface area with silver Teflon tape. For these surface radiators, the properties of silver Teflon tape are applied to the outside face of the enclosure. The bulk material, outside coating, mass, density multiplier, contact and bolt assumptions of DAC1 are included in Appendix D.

B. Heat Loads

Heat dissipations are each equally divided among the solid or surface to which they are applied, except for the thruster and those components controlled by heaters. The thruster heat load is applied to a ring of nodes within the solid cylinder of the thruster to represent the heated anode. A diagram of this is included in Appendix E. The components controlled by heaters are listed in Table 1. The maximum and minimum temperature set points of each heater were decided based on each components' temperature requirements. The Tank and PT must remain above 90°C and the FLs and PFCVs must remain above 120°C so that the iodine fuel does not solidify and clog the propulsion system. The power of each heater was selected based on what is needed to maintain the minimum set points of each heater for the Science Phase cold case. The location of the heaters and set points are also diagramed in Appendix E.

Table 1. Heater Details

Component	Heater Temperature Set Points		Power [W]
	Min [°C]	Max [°C]	
Tank	90	100	10
Pressure Transducer	90	100	2
Fuel lines	115	125	20
PFCV (each)	115	125	2

C. Phase Profiles

The power dissipation with respect to time varies for each phase. The heat dissipation details are largely defined by component specifications and the spacecraft operational timeline. It is assumed that the battery dissipates 5% of the total power at each time step, based on typical power losses of lithium ion batteries. Appendix B contains the power profile tables for each phase along with a key, which denotes the method used to determine the assumptions used to generate each component power profile.

Each phase also has a specific orientation sequence, documented in Appendix C. The possible orientations consist of Local Vertical Local Horizon (LVLH), LVLHΔ90°, and Solar Inertial. LVLH orients the satellite so that the bottom panel of the chassis, where there is a cutout for the payload lens, is always parallel to the surface of the earth, and the thrust axis is aligned with the velocity vector. LVLHΔ90° has a 90° yaw rotation from LVLH so that the bottom panel of the chassis is always parallel to the surface of the earth, but the thrust axis is not aligned with the velocity vector. Lastly, the solar inertial alignment orients the spacecraft so that the solar panels are always sun facing.

III. Environments

The orbit of the spacecraft is undefined because the launch vehicle is unknown. For this reason, the orbit parameters have been bracketed by a hot case and a cold case. The Hot Case assumes all parameters are those that produce the warmest environment for the spacecraft, which includes a dawn-dusk orbit with the spacecraft in full sun for the entire orbit. This case was analyzed with the lowest altitude, which results in more albedo heating from the earth. The Cold Case assumed all parameters are those that produce the coldest environment for the spacecraft. The orbit is a noon-midnight orbit with the spacecraft in eclipse for 37% and in view of the sun for 63% percent of the orbit. This case was analyzed with the highest altitude, which results in less albedo heating from the earth. Table 2

Table 2. Orbital Parameters for Hot and Cold Cases

Orbital Parameter	Hot Case	Cold Case
Altitude [km]	250	720
Orbit Inclination [°]	98	98
R.A. of Ascending Node [°]	295.559	27
Argument of Periapsis [°]	270	270
Calculated Beta Angle [°]	-87.911	0.075
Solar Flux [W/m ²]	1414	1322
Albedo	0.300037	0.4812
IR Planetshine [W/m ²]	239.58	218

summarizes the Hot and Cold Case orbit differences.

The hot cases analyzed for each phase were created with the hot case orbit, and using the EOL properties for the silver Teflon tape and OSR radiator optical properties. The Science phase cold case analyzed was created with the cold case orbit and using the BOL properties for the silver Teflon tape and OSR radiator optical properties.

IV. Analysis Results

Table 4 lists the components modeled, their maximum survivability and operational temperatures, the maximum temperature predicted by analysis of all phases, and during which phase the maximum temperature is predicted. If more than one phase is listed in the Phase column, then that component had the same maximum temperature in both phases. An asterisk next to a survivability or operational temperature designates that this parameter is uncertain and the designated limit is an estimate. A color key to the results is shown by Table 3. If a predicted temperature is not highlighted it is within the temperature range of the component.

Table 3. Results Table Color Key

	≥ operational temperature
	within 5°C of operational temp

Table 4. Maximum Temperatures From All Phases

Subsystem	Component Name	Max Survivability Temperature (C)	Max Operational Temperature (C)	Max Predicted Temperature (C)	Phase
Power	PMB	85	85	83	De-orbit
Power	PDB	85	85	84	De-orbit
GNC	Reaction Wheels	85	75	58	De-orbit
GNC	Star Tracker	50	50	41	De-orbit
GNC	IMU	85	85	55	De-orbit
GNC	Magnetic Torquers	85	85	54	De-orbit
GNC	GPS	95	85	53	De-orbit
GNC	GPS Antenna	100	85	52	RAAN Change, Science
GNC	Accelerometer	78	78	53	RAAN Change, De-orbit
GNC	Sun Sensor	85	75	53	RAAN Change, De-orbit
GNC	Magnetometer	85	85	48	Alt. Red.
Comm	Radio	125	85	60	De-orbit
C&DH	FC	70	60	59	De-orbit
C&DH	AB	85	85	58	De-orbit
C&DH	EIB	85	85	58	De-orbit
C&DH	Camera	150	60	36	De-orbit
Propulsion	Thruster	200	200	95, 161	De-orbit
Propulsion	PFCVs (heater)	150	130	164	Science
Propulsion	PPU	125	125	37	De-orbit
Propulsion	Cathode	450*	450*	223	Alt. Red.
Propulsion	Fuel	150*	150*	122	Alt. Red., Science
Propulsion	Tank (heater)	150*	150*	123	Science
Propulsion	Tank Insulation	200*	200*	123	Science
Propulsion	PT (heater)	100	100	109	all but RAAN
Propulsion	PT Insulation	200*	200*	109	all but RAAN
Propulsion	Fuel Lines (heater)	150*	150*	198	Alt. Red.
Propulsion	Fuel Lines Insulation	200*	200*	197	Alt. Red.
Payload	IR Camera	70	20	36	De-orbit
GNC	Ant_S	100	100	50	De-orbit
GNC	Ant_x	140	140	45	De-orbit
Power	Battery	60	60	53	De-orbit
Power	Solar Cells	110	100	83	Alt. Red.
Structure	Solar Panel PCB	110	100	83	Alt. Red.
Structure	Solar Panel Al Support	110	100	80	Alt. Red.
Structure	Chassis	120	120	60, 164	RAAN Change

V. Discussion

There are several components over their operational temperature limits and several more components within 5°C of their operation temperature limit. These unfavorable temperatures can largely be attributed to several major drivers in the thermal model: the solar panel contact details, the card stack copper heat straps, the cathode mount, and the thruster fidelity. Each of these model drivers is based on an assumption, so this does not necessarily mean that these components will overheat in flight, but it does mean that unknown details must be defined as soon as possible and the model must be updated with higher fidelity.

A. Model Drivers

The solar panel contact to which is being referred is the thermal conduction assumption between the deployable solar panel aluminum mount plate and the solar panel PCB backing. This conduction coefficient is 21 W/m²/C. The opposite side of the aluminum mountplates to which the deployable solar panels attach are the OSR radiators. The actual mounting technique of the solar panels is unknown, and this value was chosen specifically because it allows the solar panel cells to be cooled enough so that they are below the operational temperature, but does not cool them too much so that the radiators can not dissipate heat from the other components. If the value is significantly increased, the solar panels will be cooled to a lower temperature, and the temperature of the rest of the components inside the enclosure will increase. If the value is significantly decreased, however, the solar panel temperature will rise above its operational limit, but the components inside the enclosure will remain below their operational limits. Therefore, it is important to determine an appropriate design approach to attain this conduction coefficient.

The details of the card stack copper heat straps are assumed because a card stack mounting assembly has not yet been designed. It is only known that the cards will not be mounted in a closed structure. The cards were placed in the corner of the satellite so that the two adjacent sides of the cards can be used to make high contacts to the chassis through thermal straps. It was assumed that a copper strap is attached from each of those two sides on each of the circuit boards to their respective sides of the enclosure. The straps are assumed to be the minimum distance from each side of the card to the enclosure to maximize the heat transfer path from the cards. One side of each card attaches a strap 4mm long, and the other side attaches to as strap 20.6mm long. The assumed copper straps provide a good thermal contact from the cards to the chassis. The card stack mounting method is unknown, and so this good contact may not be accurate.

The cathode mount is modeled as attached to the chassis with 2 bolts. The cathode mount is contacted to the Cathode, which is then contacted to the FL. The FL must be heated continuously throughout flight to prevent the iodine fuel from clogging the propulsion system. The FL heaters, with this current mount, require a higher than expected amount of power to heat the FL to between 115 and 125 °C because much of the heat supplied to the FL is being transferred through the cathode mount and to the chassis. This mount must be isolated from the chassis or from the cathode and FL to reduce the amount of power required by the FL heaters. This will reduce heat transfer to the chassis, which will allow the chassis to absorb and dissipate heat transferred from other hot components. The cathode mount detail is shown in Figure 4.

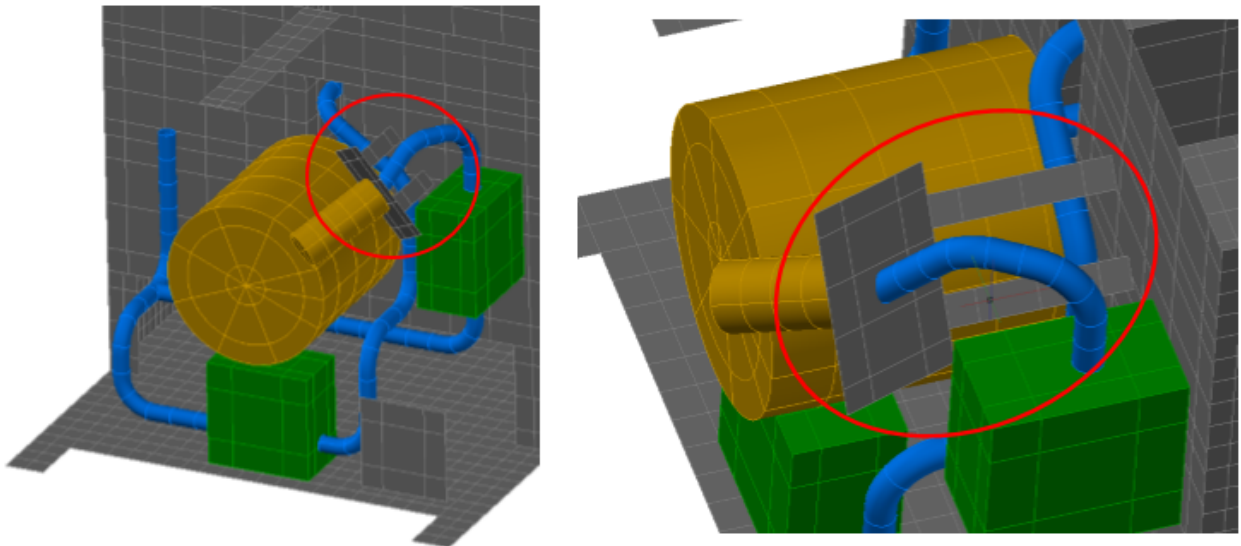


Figure 4. Cathode Mount Detail

The thruster is modeled as a solid cylinder of carbon phenolic with a density multiplier applied to mimic the actual mass of the thruster. This is very much simplified from the actual design of the thruster. The solid aspect of the model allows for the heat to distribute throughout the thruster, whereas in the actual thruster there will likely be isolated hot and cold areas. These areas are of importance because the temperature limit of the thruster magnetic coils is 200°C. Currently, the model does not go over 200°C, but a higher fidelity model may have an isolated hot spot over that limit. Figure 5 shows the current thruster TD model and a drawing of the actual thruster, for comparison.

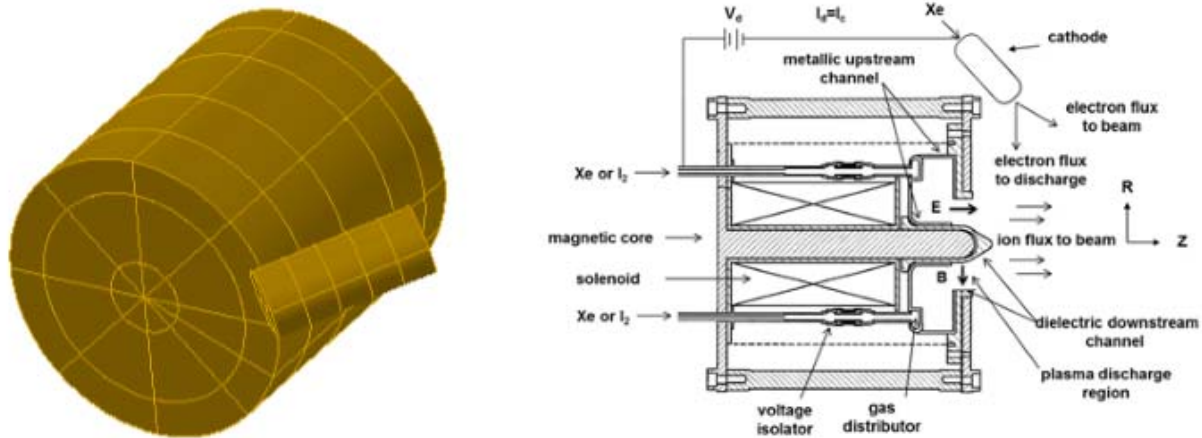


Figure 5. Low Fidelity TD Model (left) and High Fidelity Drawing (Right) of Thruster

B. Over-temp Components

The component temperatures above or within 5°C of their survival temperature are summarized in Table 5.

Table 5. Over-Temp Components of the Hot Cases

Subsystem	Component Name	Max Survivability Temperature (C)	Max Operational Temperature (C)	Max Predicted Temperature (C)
Power	PMB	85	85	83
Power	PDB	85	85	84
C&DH	FC	70	60	59
Propulsion	PFCVs (heater)	150	130	164
Propulsion	PT (heater)	100	100	109
Propulsion	Fuel Lines (heater)	150*	150*	198
Propulsion	Fuel Lines Insulation	200*	200*	197
Payload	IR Camera	70	20	36
Power	Battery	60	60	53
Structure	Chassis	120	120	60, 164

The PMB and PDB are over-temp partially because they are the two circuit boards dissipating the most heat. The most that the PMB and PDB dissipate is 12W and 12.46W, respectively. The Flight Computer is of concern because its operational temperature limit is 60°C, whereas the other circuit boards have a limit of 85°C. The high temperatures of these boards reinforce the importance of the card stack mounting. The model currently assumes that very good heat straps are being used, which contributes to these temperatures not being higher.

Both PFCVs and FLs are above their operational temperature limits. This can partially be attributed to the Cathode mount and FL contact assumptions. Because the heat from the FLs is being transferred to the chassis, the FL nodes closest to the mount are dropping below the heater minimum set point of 115°C, which is causing the FL heater to remain on because it senses the temperature from the minimum temperature node. Therefore, the nodes of the FL that are not having heat drawn away through the cathode mount are overheating, which is then heating the PFCVs. This is also why the FL insulation is nearing its operational limit. The chassis temperature is also over its operational limit of 120°C on the cathode mount, when the cathode is firing. The highest temperature of the chassis, not including the cathode mount, is less than half of what the mount reaches. Isolating the cathode and FLs from the cathode mount, and using multiple zones to control the heaters will decrease these temperatures.

The PT is above its operational temperature limit because the current PT requires an operational temperature below 100°C, but the iodine fuel needs to be heated above at least 90°C, and the heater set points are 90 to 100°C.

The tank is being heated by the over-heated fuel lines, and thus heating the PT above its limit. The PT temperature may also be reduced by isolating the FLs.

The Battery temperature is not within 5°C of its operational temperature, but it is known that if the battery operates in the currently predicted temperatures its efficiency is greatly decreased and will not survive the entire year long mission. It is favorable for the battery to be closer to 30-35°C.

The Payload LWIR Camera is also above its operational limit. The payload is only operating during the Science Phase, but during that phase the camera is also above its operational limit of 20°C at 32°C. Because the rest of the components and the enclosure are above this temperature, it is unlikely that a copper thermal strap will further reduce the payload temperatures. The temperatures of the enclosure need to be reduced to be able to also reduce the payload temperatures.

VI. DAC2 Model Changes

Many model changes have been made during the second Design and Analysis Cycle (DAC2), which encompasses changes made in the five months after Preliminary Design Review (PDR). The model changes are a result of both spacecraft configuration changes, and of increased model fidelity based on further definition of components since DAC1 and imposed requirements.

A. iSAT Configuration Changes

Changes included in the preliminary analysis for DAC2 include:

- Removal of solar array body array, which was attached directly to the chassis
- Relocation of side deployable solar panels to deploy from back deployable solar panel, rather than from chassis
- Requirement imposed that fuel lines be thermally isolated from thruster connection and cathode connection
- Requirement imposed that cathode be thermally isolated from cathode mount
- All insulation changed to high temperature single layer insulation
- Fuel line heaters increased from one to three.

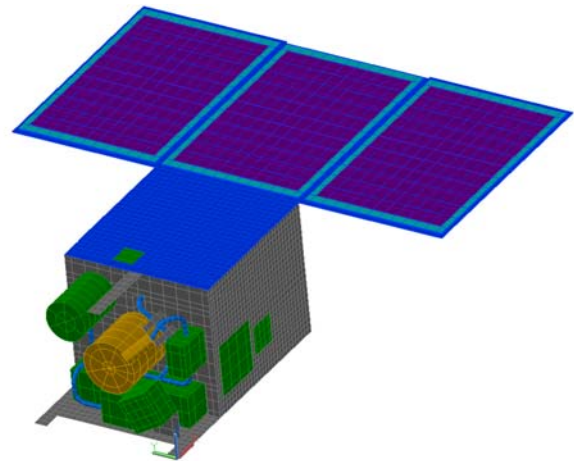


Figure 6. Outside view of DAC2 Preliminary Changes TD Model

Figure 6 shows the outside view of the DAC2 TD model with these changes made. Figure 1 shows the DAC1 model for comparison.

B. Increased Model Fidelity

A high fidelity thruster model has also been created using Thermal Desktop and imported into the integrated spacecraft model. A model with the low fidelity thruster replaced with the high fidelity version was analyzed and compared to the same model with the thruster fidelity being the only difference. This comparison showed that the thruster model change affected the other component temperatures by only a 1 to 2°C difference. Because of the small difference, next iterations of the design will keep the low fidelity thruster because model run time is much faster. The high fidelity thruster model also showed that the thruster was not in danger of exceeding its maximum operational temperatures with its current power distribution and requirements.

C. DAC2 Preliminary Analysis Results

Table 6 lists the components modeled, their maximum survivability and operational temperatures, and the maximum temperature predicted by DAC1 and DAC2 analysis for the hot case of the Altitude Reduction Phase. Due to time constraints, this is the only phase modeled thus far. An asterisk next to a survivability or operational temperature designates that this parameter is untested and the designated limit is an estimate. A color key is shown by Table 3. If a predicted temperature is not highlighted it is within the temperature range of the component. Some survivability and operational temperatures have been updated since the DAC1 analysis results and are not the same as shown in Table 4.

Table 6. DAC1 vs. DAC2 Altitude Reduction Phase Results

Subsystem	Component Name	Max Survivability Temperature (C)	Max Operational Temperature (C)	Maximum Analysis Temperature (C)	
				DAC1	DAC2
Power	PMB	85	85	79	62
Power	PDB	85	85	76	58
GNC	Reaction Wheels	85	75	51	31
GNC	Star Tracker	50	50	33	17
GNC	IMU	85	85	46	18
GNC	Magnetic Torquers	85	85	50	30
GNC	GPS	95	85	47	19
GNC	GPS Antenna	100	85	46	20
GNC	Accelerometer	78	78	47	20
GNC	Sun Sensor	85	75	48	19
GNC	Magnetometer	85	85	48	13
Comm	Radio	125	85	59	32
C&DH	FC	70	60	55	39
C&DH	AB	85	85	50	30
C&DH	EIB	85	85	50	29
C&DH	Camera	150	60	31	18
Propulsion	Thruster... Anode	200	200	89... 150	69, 140
Propulsion	PFCVs (heater)	150	130	162	124
Propulsion	PFCVs Insulation	400	290	162	124
Propulsion	PPU	125	125	30	15
Propulsion	Cathode	450*	450*	223	204
Propulsion	Fuel	150*	150*	122	111
Propulsion	Tank (heater)	150*	150*	122	113
Propulsion	Tank Insulation	400	290	122	114
Propulsion	PT (heater)	100	100	109	93
Propulsion	PT Insulation	400	290	109	93
Propulsion	Fuel Lines (heater)	150*	150*	198	141
Propulsion	Fuel Lines Insulation	400	290	197	140
Payload	IR Camera	70	20	32	16
GNC	Ant_S	100	100	43	20
GNC	Ant_x	140	140	40	18
Power	Battery	60	60	43	19
Power	Solar Cells	110	100	83	83
Structure	Solar Panel PCB	110	100	83	84
Structure	Solar Panel Al Support	110	100	80	79
Structure	Chassis Main... Cathode Mount	120*	120*	56... 124	35, 104

D. Discussion

The major drop in temperatures is caused by the removal of the body array solar panel and the relocation of the side deployable solar panels to deploy from the back deployable solar panel, rather than from the chassis. Removing the body array removes a heat source that was transferring heat directly into the chassis, and thus chassis mounted components, and also increases the radiative surface area of the enclosure. Relocating the side deployable solar panels also removes a heat source that was transferring heat directly into the chassis. This change increases the efficiency of both the radiators on the back side of the solar panels, and the radiative surface area of the enclosure, because these two surfaces no longer view each other at a 90° angle, allowing a better view to space. These two changes isolate the solar panels from the rest of the spacecraft, allowing the solar panels to more effectively cool themselves with the radiators on the backside of the deployable panels. This also allows the chassis to more effectively cool itself and the components inside with the enclosure radiator surfaces. The new configuration reduces the impact of the solar panels' designs to impact internal chassis mounted hardware.

The fuel lines temperatures have been reduced because the fuel lines have been isolated from both the thruster and the cathode by assuming the contact bolts are using ceramic washers. The requirement to thermally isolate the fuel lines has been imposed on the propulsion mounting method to properly heat the fuel lines. Because the thruster and cathode are no longer acting as heat sinks to draw the heat away from the fuel lines, the heaters require less

power to heat the fuel lines to the required temperature. The enclosure temperature of the cathode mount was reduced because the cathode is also isolated from the cathode mount.

As a final design change, the fuel lines, valves, and tank insulation was modified to allow for higher operational temperature limits and is no longer a design concern. This insulation selected is Sheldahl Aluminum Coated Black Kapton, which has a higher maximum operational limit, and so the overheating of the insulation is no longer a concern.

VII. Upcoming Work

Further configuration changes will be made as part of DAC2, including:

- Removal of pressure transducer
- Removal of accelerometer
- Removal of X-band antenna
- Change of radio – to separate receiver and transmitter and only S-band antenna
- Larger momentum wheels
- Relocation of most components

Additional fidelity must also be added to individual components to decrease the uncertainty of the current model. Much of this fidelity is not already in the model because the components concerned are not yet selected or fully defined.

- Component to chassis contact update: to determine contact values based on specific bolt type and torque rather than a typical contact value
- Deployable solar panel to chassis contact update: this hinge is currently being designed.
- Solar panel details: solar panels are currently being designed.
- The battery will likely be modeled in high fidelity since its temperature determines its efficiency and thus affects the number of solar panels required.
- Card stack mounting scheme: The method of mounting the card stack and whether thermal straps will be used is being assessed.

Additional phases of the mission will be analyzed in both hot and cold cases, along with a variation in several random beta angles verify that there are no worst case beta angle conditions. A start-up mode and safe mode will also be analyzed to evaluate the the colder environments experienced when not all spacecraft components are powered on.

Throughout the upcoming work planned, the thermal results and conclusions will be shared with design, stress, and other disciplines to verify requirements of all disciplines can be met with each changing iteration.

VIII. Conclusion

The thermal design and analysis of iSAT has been challenging due to the high power density of the spacecraft. It is a very small spacecraft and needs to dissipate a very large amount of power. Containing components with high sensitivity to temperature, such as the battery, flight computer, and payload LWIR, adds an additional level of difficulty. Strides have been made in the spacecraft design to reduce temperatures by changing the solar panel configuration, but this does not resolve all of the thermal concerns. Additional concerns are related to the lack of fidelity of components chosen or mounting methods, such as the card stack mounting methods. The spacecraft design, component locations, and thermal systems will continue to change and evolve as the design matures and final components are selected and the configuration solidified.

IX. Acknowledgments

The author would like to thank the iSAT team and mentors for all working hard on this project and always being open to answering questions. An extended thanks is given to Rob Coker, the author's mentor for the project, Shawn Breeding and Brian O'Connor, to whom many thermal questions were directed, and to Patrick Hull, Joao Seixial, and Adam Burt, who comprise the remainder of the Mechanical Design and Analysis team.

X. References

¹Thermal Desktop, Ver.5.6 Patch 8, Cullimore & Ring (C&R) Technologies, Inc.

²SINDA/FLUINT, Ver.5.5 Patch 11, Cullimore & Ring (C&R) Technologies, Inc.

XI. Appendix

A. Additional Images of the DAC1 Model

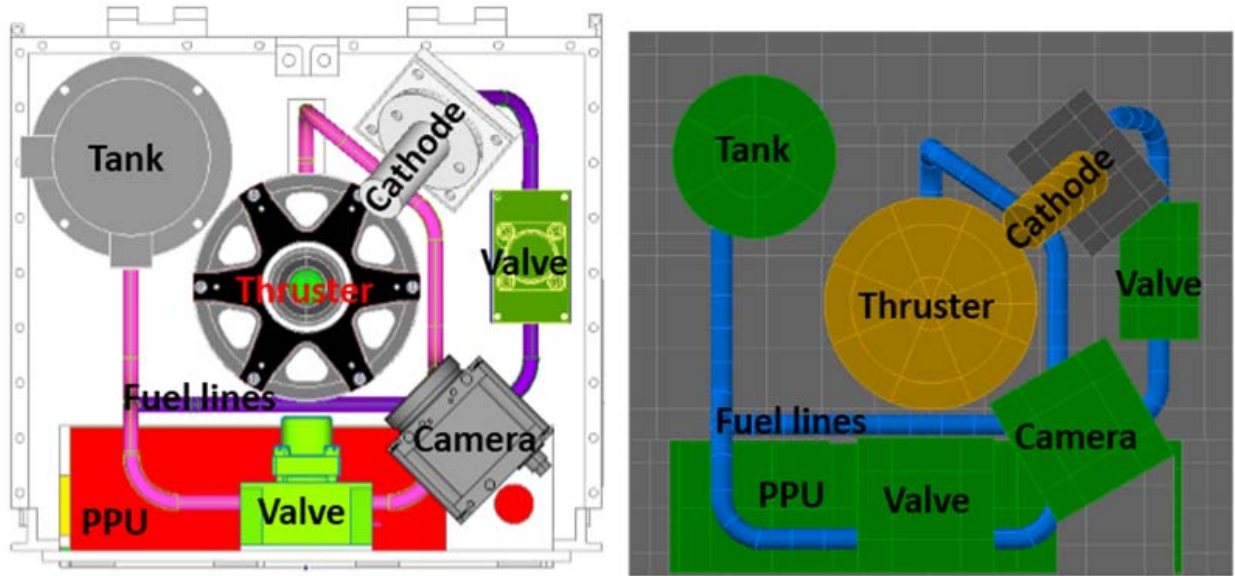


Figure 7: Front of Spacecraft Showing Propulsion System in CAD (left) and TD (right)

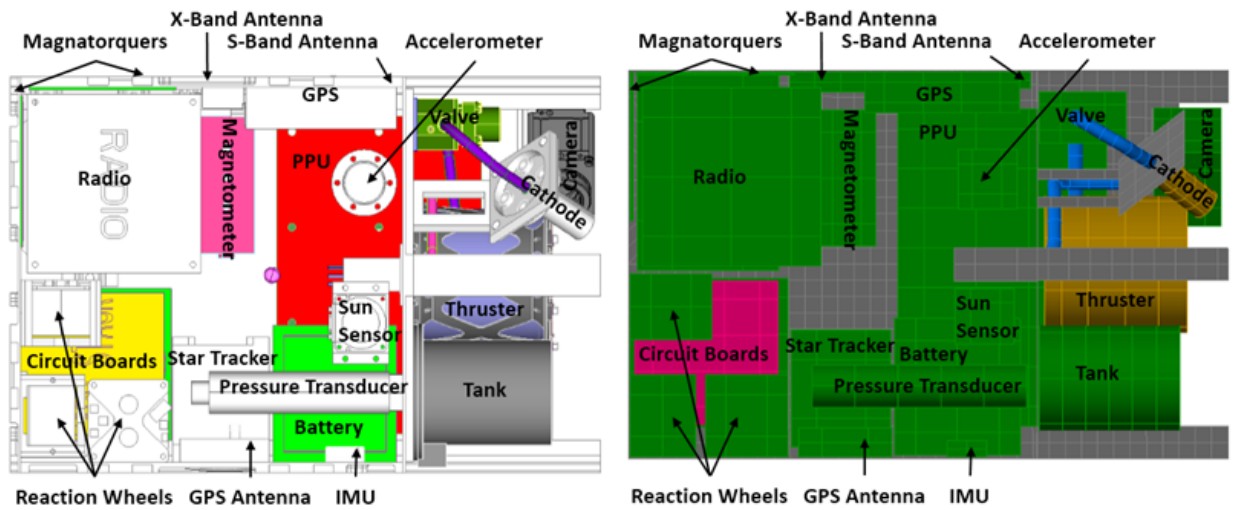


Figure 8: Top View of Spacecraft in CAD (left) and TD (right)

B. Power Profiles for Each Modeled Phase

Table 2. Power Profile Key

	Available heater power
	Calculated based on cathode/anode split
	Component Specifications / SC Operational Timeline

Table 8. RAAN Change Phase Power Profile

	Power Dissipation per unit during State (W) over 1 orbit						
	State	Remaining Eclipse Time	Firing (6 min burn mode)	Remaining Eclipse Time	Comm Pass	Charging	Charging + Momentum Dump
	Length of State [s]	540	360	540	540	1080	2880
	Time at end of State [s]	540	900	1440	1980	3060	5940
Subsystem	Component Name						
Power	PMB	OFF	OFF	OFF	OFF	12.00	12.00
Power	PDB	8.21	11.79	8.21	12.46	8.21	8.68
GNC	Reaction Wheels	0.10	0.40	0.10	0.10	0.10	0.10
GNC	Star Tracker	1.00	1.00	1.00	1.00	1.00	1.00
GNC	IMU	0.10	0.10	0.10	0.10	0.10	0.10
GNC	Magnetic Torquers	OFF	OFF	OFF	OFF	OFF	0.63
GNC	GPS	1.20	1.20	1.20	1.20	1.20	1.20
GNC	GPS Antenna	0.06	0.06	0.06	0.06	0.06	0.06
GNC	Accelerometer	0.48	0.48	0.48	0.48	0.48	0.48
GNC	Sun Sensor	0.08	0.08	0.08	0.08	0.08	0.08
GNC	Magnetometer	0.40	0.40	0.40	0.40	0.40	0.40
Comm	Radio	OFF	OFF	OFF	16.00	OFF	OFF
C&DH	FC	4.80	4.80	4.80	4.80	4.80	4.80
C&DH	AB	0.79	0.79	0.79	0.79	0.79	0.79
C&DH	EIB	0.79	0.79	0.79	0.79	0.79	0.79
C&DH	Camera	OFF	3.10	OFF	OFF	OFF	OFF
Propulsion	Thruster	OFF	65.03	OFF	OFF	OFF	OFF
Propulsion	PFCVs	2.00	2.00	2.00	2.00	2.00	2.00
Propulsion	PPU	0.48	18.88	0.48	0.48	0.48	0.48
Propulsion	Cathode	OFF	62.03	OFF	OFF	OFF	OFF
Propulsion	Tank Heater	10.00	10.00	10.00	10.00	10.00	10.00
Propulsion	PTs	2.00	2.00	2.00	2.00	2.00	2.00
Propulsion	Prop Line Heaters	20.00	20.00	20.00	20.00	20.00	20.00
Payload	IR Camera	OFF	OFF	OFF	OFF	OFF	OFF

Table 9. Altitude Reduction Phase Power Profile

Power Dissipation per unit during State (W) over 3 orbits								
State	Eclipse	Firing (6 min burn mode)	Eclipse	Comm Pass	Charging	Charging + Momentum Dump	Eclipse	
Length of State [s]	540	360	540	540	1080	2880	1440	
Time at end of State [s]	540	900	1440	1980	3060	5940	7380	
Subsystem	Component Name							
Power	PMB	OFF	OFF	OFF	OFF	12.00	12.00	OFF
Power	PDB	8.21	11.79	8.21	12.46	8.21	8.68	8.21
GNC	Reaction Wheels	0.10	0.40	0.10	0.10	0.10	0.10	0.10
GNC	Star Tracker	1.00	1.00	1.00	1.00	1.00	1.00	1.00
GNC	IMU	0.10	0.10	0.10	0.10	0.10	0.10	0.10
GNC	Magnetic Torquers	OFF	OFF	OFF	OFF	OFF	0.63	OFF
GNC	GPS	1.20	1.20	1.20	1.20	1.20	1.20	1.20
GNC	GPS Antenna	0.06	0.06	0.06	0.06	0.06	0.06	0.06
GNC	Accelerometer	0.48	0.48	0.48	0.48	0.48	0.48	0.48
GNC	Sun Sensor	0.08	0.08	0.08	0.08	0.08	0.08	0.08
GNC	Magnetometer	0.40	0.40	0.40	0.40	0.40	0.40	0.40
Comm	Radio	OFF	OFF	OFF	16.00	OFF	OFF	OFF
C&DH	FC	4.80	4.80	4.80	4.80	4.80	4.80	4.80
C&DH	AB	0.79	0.79	0.79	0.79	0.79	0.79	0.79
C&DH	EIB	0.79	0.79	0.79	0.79	0.79	0.79	0.79
C&DH	Camera	OFF	3.10	OFF	OFF	OFF	OFF	OFF
Propulsion	Thruster	OFF	65.03	OFF	OFF	OFF	OFF	OFF
Propulsion	PFCVs	2.00	2.00	2.00	2.00	2.00	2.00	2.00
Propulsion	PPU	0.48	18.88	0.48	0.48	0.48	0.48	0.48
Propulsion	Cathode	OFF	62.03	OFF	OFF	OFF	OFF	OFF
Propulsion	Tank Heater	10.00	10.00	10.00	10.00	10.00	10.00	10.00
Propulsion	PTs	2.00	2.00	2.00	2.00	2.00	2.00	2.00
Propulsion	Prop Line Heaters	20.00	20.00	20.00	20.00	20.00	20.00	20.00
Payload	IR Camera	OFF	OFF	OFF	OFF	OFF	OFF	OFF
Power Dissipation per unit during State (W) over 3 orbits continued...								
Comm Pass	Charging	Firing (6 min burn mode)	Charging	Eclipse	Comm Pass	Charging	Charging + Momentum Dump	
540	1350	360	2250	1440	540	1080	2880	
7920	9270	9630	11880	13320	13860	14940	17820	
OFF	12.00	OFF	12.00	OFF	OFF	12.00	12.00	
12.46	8.21	11.79	8.21	8.21	12.46	8.21	8.68	
0.10	0.10	0.40	0.10	0.10	0.10	0.10	0.10	
1.00	1.00	1.00	1.00	1.00	1.00	1.00	1.00	
0.10	0.10	0.10	0.10	0.10	0.10	0.10	0.10	
OFF	OFF	OFF	OFF	OFF	OFF	OFF	0.63	
1.20	1.20	1.20	1.20	1.20	1.20	1.20	1.20	
0.06	0.06	0.06	0.06	0.06	0.06	0.06	0.06	
0.48	0.48	0.48	0.48	0.48	0.48	0.48	0.48	
0.08	0.08	0.08	0.08	0.08	0.08	0.08	0.08	
0.40	0.40	0.40	0.40	0.40	0.40	0.40	0.40	
16.00	OFF	OFF	OFF	OFF	16.00	OFF	OFF	
4.80	4.80	4.80	4.80	4.80	4.80	4.80	4.80	
0.79	0.79	0.79	0.79	0.79	0.79	0.79	0.79	
0.79	0.79	0.79	0.79	0.79	0.79	0.79	0.79	
OFF	OFF	3.10	OFF	OFF	OFF	OFF	OFF	
OFF	OFF	65.03	OFF	OFF	OFF	OFF	OFF	
2.00	2.00	2.00	2.00	2.00	2.00	2.00	2.00	
0.48	0.48	18.88	0.48	0.48	0.48	0.48	0.48	
OFF	OFF	62.03	OFF	OFF	OFF	OFF	OFF	
10.00	10.00	10.00	10.00	10.00	10.00	10.00	10.00	
2.00	2.00	2.00	2.00	2.00	2.00	2.00	2.00	
20.00	20.00	20.00	20.00	20.00	20.00	20.00	20.00	
OFF	OFF	OFF	OFF	OFF	OFF	OFF	OFF	

Table 3. De-orbit Phase Power Profile

Power Dissipation per unit during State (W) over 1 orbit							
State	Remaining Eclipse Time	Firing (6 min burn mode)	Remaining Eclipse Time	Comm Pass	Charging	Charging + Momentum Dump	
Length of State [s]	540	360	540	540	1080	2880	
Time at end of State [s]	540	900	1440	1980	3060	5940	
Subsystem	Component Name						
Power	PMB	OFF	OFF	OFF	OFF	12.00	12.00
Power	PDB	8.21	11.79	8.21	12.46	8.21	8.68
GNC	Reaction Wheels	0.10	0.40	0.10	0.10	0.10	0.10
GNC	Star Tracker	1.00	1.00	1.00	1.00	1.00	1.00
GNC	IMU	0.10	0.10	0.10	0.10	0.10	0.10
GNC	Magnetic Torquers	OFF	OFF	OFF	OFF	OFF	0.63
GNC	GPS	1.20	1.20	1.20	1.20	1.20	1.20
GNC	GPS Antenna	0.06	0.06	0.06	0.06	0.06	0.06
GNC	Accelerometer	0.48	0.48	0.48	0.48	0.48	0.48
GNC	Sun Sensor	0.08	0.08	0.08	0.08	0.08	0.08
GNC	Magnetometer	0.40	0.40	0.40	0.40	0.40	0.40
Comm	Radio	OFF	OFF	OFF	16.00	OFF	OFF
C&DH	FC	4.80	4.80	4.80	4.80	4.80	4.80
C&DH	AB	0.79	0.79	0.79	0.79	0.79	0.79
C&DH	EIB	0.79	0.79	0.79	0.79	0.79	0.79
C&DH	Camera	OFF	3.10	OFF	OFF	OFF	OFF
Propulsion	Thruster	OFF	65.03	OFF	OFF	OFF	OFF
Propulsion	PFCVs	2.00	2.00	2.00	2.00	2.00	2.00
Propulsion	PPU	0.48	18.88	0.48	0.48	0.48	0.48
Propulsion	Cathode	OFF	62.03	OFF	OFF	OFF	OFF
Propulsion	Tank Heater	10.00	10.00	10.00	10.00	10.00	10.00
Propulsion	PTs	2.00	2.00	2.00	2.00	2.00	2.00
Propulsion	Prop Line Heaters	20.00	20.00	20.00	20.00	20.00	20.00
Payload	IR Camera	OFF	OFF	OFF	OFF	OFF	OFF

Table 4. Science Phase Power Profile

Power Dissipation per unit during State (W) over 1 orbit				
State	Remaining Eclipse Time	Firing (6 min burn mode)	Remaining Eclipse Time	
Length of State [s]	1440	540	3960	
Time at end of State [s]	1440	1980	5940	
Subsystem	Component Name			
Power	PMB	OFF	OFF	12.00
Power	PDB	8.71	12.46	8.21
GNC	Reaction Wheels	0.10	0.10	0.10
GNC	Star Tracker	1.00	1.00	1.00
GNC	IMU	0.10	0.10	0.10
GNC	Magnetic Torquers	OFF	OFF	OFF
GNC	GPS	1.20	1.20	1.20
GNC	GPS Antenna	0.06	0.06	0.06
GNC	Accelerometer	0.48	0.48	0.48
GNC	Sun Sensor	0.08	0.08	0.08
GNC	Magnetometer	0.40	0.40	0.40
Comm	Radio	OFF	16.00	OFF
C&DH	FC	4.80	4.80	4.80
C&DH	AB	0.79	0.79	0.79
C&DH	EIB	0.79	0.79	0.79
C&DH	Camera	OFF	OFF	OFF
Propulsion	Thruster	OFF	OFF	OFF
Propulsion	PFCVs	2.00	2.00	2.00
Propulsion	PPU	0.48	0.48	0.48
Propulsion	Cathode	OFF	OFF	OFF
Propulsion	Tank Heater	2.00	2.00	2.00
Propulsion	PTs	10.00	10.00	10.00
Propulsion	Prop Line Heaters	20.00	20.00	20.00
Payload	IR Camera	2.00	OFF	OFF

C. Space Craft Orientation for Each Modeled Phase

Table 5. RAAN Change Phase Spacecraft Orientation

RAAN Phase Change State	Remaining Eclipse Time	Firing (6 min burn mode)	Remaining Eclipse Time	Comm Pass	Charging	Charging + Momentum Dump
Length of State [s]	540	360	540	540	1080	2880
Time at end of State [s]	540	900	1440	1980	3060	5940
Orientation	Solar Inertial	LVLH $\Delta 90^\circ$	Solar Inertial	LVLH	Solar Inertial	Solar Inertial

Table 6. Altitude Reduction Phase Spacecraft Orientation

Altitude Reduction Phase State	Eclipse	Firing (6 min burn mode)	Eclipse	Comm Pass	Charging	Charging + Momentum Dump	Eclipse
Length of State [s]	540	360	540	540	1080	2880	1440
Time at end of State [s]	540	900	1440	1980	3060	5940	7380
Orientation	Solar Inertial	LVLH	Solar Inertial	LVLH	Solar Inertial	Solar Inertial	Solar Inertial
	Comm Pass	Charging	Firing (6 min burn mode)	Charging	Eclipse	Comm Pass	Charging
	540	1350	360	2250	1440	540	1080
	7920	9270	9630	11880	13320	13860	14940
	LVLH	Solar Inertial	LVLH	Solar Inertial	Solar Inertial	LVLH	Solar Inertial
							Charging + Momentum Dump
							2880
							17820

Table 7. De-orbit Phase Spacecraft Orientation

De-orbit Phase State	Remaining Eclipse Time	Firing (6 min burn mode)	Remaining Eclipse Time	Comm Pass	Charging	Charging + Momentum Dump
Length of State [s]	540	360	540	540	1080	2880
Time at end of State [s]	540	900	1440	1980	3060	5940
Orientation	Solar Inertial	LVLH	Solar Inertial	LVLH	Solar Inertial	Solar Inertial

Table 8. Science Phase Spacecraft Orientation

Science Phase State	Remaining Eclipse Time	Firing (6 min burn mode)	Remaining Eclipse Time
Length of State [s]	1440	540	3960
Time at end of State [s]	1440	1980	5940
Orientation	LVLH	LVLH	Solar Inertial

D. DAC1 Component TD Model Details

Table 9. Component Model and Master Equipment List (MEL) Masses and Density Multipliers

Component	MEL Mass [kg]	Model Mass [kg]	Density Multiplier Calculated
Primary Structures	3.500	3.57	2.51
Secondary Structures	1.500	0.575	1
Card Stack Hardware	0.021	Not included	
Solar Array Deployment Mechanism	0.250	Not included	
Support Systems	0.056	Not included	
Insulation	0.000	1.3975	1
Solar Panel - Deployed	0.799	0.992	1
Solar Panel - Body Mount	0.092	0.118	2.51
Power Management Board	0.060	0.06	0.7
Power Distribution Board	0.060	0.06	0.7
Battery	1.123	1.123	0.88
Reaction Wheel	0.555	0.534	0.66
Star Tracker	0.159	0.159	0.2
IMU	0.007	0.007	0.54
Magnetic Torquers	0.090	0.09	0.77
GPS Receiver	0.165	0.165	0.57
GPS Antenna	0.082	0.079	0.52
Accelerometer	0.075	0.072	0.26
Sun Sensor	0.040	0.0385	0.58
Magnetometer	0.100	0.096	0.39
Radio	1.400	1.681	1
X-Band Antenna	0.030	0.03	0.53
S-Band Antenna	0.085	0.085	0.5
Flight Computer	0.094	0.094	1.1
Auxiliary Board	0.116	0.116	1.36
Extra Interface Board	0.116	0.116	1.36
Camera	0.175	0.168	0.55
Separation Sensor	0.160	Not included	
Separation Electrical Connector	0.011	Not included	
Thruster	0.990	0.99	1.49
Proportional Flow Control Valve	0.455	0.461	0.33
Power Processing Unit	1.400	1.4	0.51
Cathode	0.130	0.13	4.67
Tank	0.200	0.285	2.75
Fill/Drain Plug	0.050	Not included	
Pressure Transducer	0.142	0.144	0.27
RTD	0.050	Not included	
Propellant Lines	0.168	0.05	1
Propellant Line Heaters	0.080	Not included	
Cable Harness	1.492	Not included	
LWIR	0.950	0.914	0.47
"Selfie Sat" Display	0.002	Not included	
Iodine Diagnostics	0.024	Not included	
Solid Iodine	0.700	0.702	0.83

Table 10. Thermophysical Properties of Components

Component	Bulk Material	Conductivity [W/m/°C]	Density [kg/m ³]	Heat Capacity [J/kg/°C]
Primary Structures	AL 7075-T73	155.77	2823.35	958.78
Secondary Structures	Al 7075-T6 MPDB	124.386*	2795.23	847.196*
Card Stack Hardware	Not included			
Solar Array Deployment Mechanism	Not included			
Support Systems	Not included			
Insulation (Fuellines, PT, Tank)	1mm MLI03	20.77	27679.90	4186.80
Solar Panel PCB Mount	PCB 0.2%	1.12	1951.99	1597.57
Solar Panel Cells	PCB 4.6%	18.04	2259.77	1544.11
Power Management Board	PCB 4.6%	18.04	2259.77	1544.11
Power Distribution Board	PCB 4.6%	18.04	2259.77	1544.11
Battery	PCB 4.6%	18.04	2259.77	1544.11
Reaction Wheel	Al 6061-T6 MIL	151.517*	2711.93	872.864*
Star Tracker	PCB 4.6%	18.04	2259.77	1544.11
IMU	PCB 4.6%	18.04	2259.77	1544.11
Magnetic Torquers	PCB 4.6%	18.04	2259.77	1544.11
GPS Receiver	PCB 4.6%	18.04	2259.77	1544.11
GPS Antenna	Al 6061-T6 MIL	151.517*	2711.93	872.864*
Accelerometer	SST 300	14.64	8000.00	502.10
Sun Sensor	Al 6061-T6 MIL	151.517*	2711.93	872.864*
Magnetometer	Al 5052	142.06	2684.69	921.10
Radio Circuit Boards	PCB 4.6% (boards)	18.04	2259.77	1544.11
Radio Enclosure	Al 6061-T6 MIL	151.517*	2711.93	872.864*
X-Band Antenna	PCB 4.6%	18.04	2259.77	1544.11
S-Band Antenna	PCB 4.6%	18.04	2259.77	1544.11
Flight Computer	PCB 4.6%	18.04	2259.77	1544.11
Auxiliary Board	PCB 4.6%	18.04	2259.77	1544.11
Extra Interfaces Board	PCB 4.6%	18.04	2259.77	1544.11
Camera	Al 6061-T6 MIL	151.517*	2711.93	872.864*
Separation Sensor	Not included			
Separation Electrical Connector	Not included			
Thruster	Carbon Phenolic	1.32	1435.90	1085.73
Proportional Flow Control Valve	SST 300	14.64	8000.00	502.10
Power Processing Unit	PCB 4.6%	18.04	2259.77	1544.11
Cathode	Graphite	112.15	2162.64	712.00
Tank	Titanium	7.09	4428.78	539.57
Fill/Drain Plug	Not included			
Pressure Transducer	SST 300	14.64	8000.00	502.10
RTD	Not included			
Propellant Lines	Al 6061-T6 MIL			
Propellant Line Heaters	Not included			
Cable Harness	Not included			
LWIR	Al 6061-T6 MIL	151.517*	2711.93	872.864*
"Selfie Sat" Display	Not included			
Iodine Diagnostics	Not included			
Solid Iodine	Iodine	0.45	4940.00	429.00

Table 11. Optical Properties of Components

Component	Optical Coating	Emissivity	Absorptivity
Primary Structures: outside BOL	Silver Teflon Tape BOL	0.87	0.09
Primary Structures: outside EOL	Silver Teflon Tape EOL	0.83	0.13
Primary Structures: inside	Black Anodized	0.88	0.88
Secondary Structures: top	Alodine Aluminum	0.12	0.45
Secondary Structures: bottom BOL	Optical Solar Radiator (OSR) BOL	0.8	0.07
Secondary Structures: bottom EOL	Optical Solar Radiator (OSR) EOL	0.78	0.12
Card Stack Hardware	Not included		
Solar Array Deployment Mechanism	Not included		
Support Systems	Not included		
Insulation (Fuellines, PT, Tank)	Aluminum on Black Kapton	0.03	0.12
Solar Panel PCB Mount	PCB	0.93	1
Solar Panel Cells	Inactive Panel	0.84	0.92
Power Management Board	PCB	0.93	1
Power Distribution Board	PCB	0.93	1
Battery	Al 6061-T6 MIL	0.3	0.8
Reaction Wheel	Gold	0.025	0.075
Star Tracker	Black Anodized	0.88	0.88
IMU	Al 6061-T6 MIL	0.3	0.8
Magnetic Torquers	PCB	0.93	1
GPS Receiver	Al 6061-T6 MIL	0.3	0.8
GPS Antenna	2 Layer Polyethylene Film	0.183	0.075
Accelerometer	SST Machine Rolled	0.11	0.39
Sun Sensor	Gold	0.075	0.025
Magnetometer	Al 6061-T6 MIL	0.3	0.8
Radio Circuit Boards	PCB	0.93	1
Radio Enclosure inside & outside	Black Anodized	0.88	0.88
S-Band Antenna Inside	Ant_inside	0.82	0.39
S-Band Antenna outside	Ant_outside	0.8	0.8
X-Band Antenna Inside	Ant_inside	0.82	0.39
X-Band Antenna outside	Ant_outside	0.8	0.8
Flight Computer	PCB	0.93	1
Auxiliary Board	PCB	0.93	1
Extra Interfaces Board	PCB	0.93	1
Camera	Al 6061-T6 MIL	0.3	0.8
Separation Sensor	Not included		
Separation Electrical Connector	Not included		
Thruster face	Ceramic	0.2	0.5
Thruster all other sides	White Paint	0.92	0.17
Proportional Flow Control Valve	SST Machine Rolled	0.11	0.39
Power Processing Unit	Black Anodized	0.88	0.88
Cathode	Graphite	0.85	0.88
Tank	See Insulation		
Fill/Drain Plug	Not included		
Pressure Transducer	See Insulation		
RTD	Not included		
Propellant Lines	See Insulation		
Propellant Line Heaters	Not included		
Cable Harness	Not included		
LWIR	Al 6061-T6 MIL	0.3	0.8
"Selfie Sat" Display	Not included		
Iodine Diagnostics	Not included		
Solid Iodine	N/A		

Table 12. TD Model Contacts Using conduction coefficient per Area

Component From	Component To	Conduction Coefficient (Conductance/Area) [W/m²/C]	Contact Form (face or edge)
Solar Cells	Solar Panel PCB Support	2839	face
Solar Panel Al Mount	Solar Panel PCB Support	21	face
Battery	Chassis	default	face
Reaction Wheels	Chassis	default	face
Star Tracker	Chassis	default	face
IMU	Chassis	default	face
Magnetic Torquers	Chassis	default	face
GPS Receiver	Chassis	default	face
GPS Antenna	Chassis	default	face
Magnetometer	Chassis	default	face
Accelerometer	Chassis	default	face
Radio	Chassis	default	face
X-Band Antenna	Chassis	default	face
S-Band Antenna	Chassis	default	face
Camera	Mount	default	face
Power Processing Unit	Chassis	default	face
Tank shell bottom	Pressure Transducer	default	face
Fuel Lines	Valves	3270	face
	Tank	3270	face
Payload: LWIR	Chassis	default	face
Solid Iodine	Tank Shell Sides	default	face

Table 20. TD Model Contacts Using Material Between Components

Component From	Component To	Coefficient (Thickness of Contact/Length through Material)	Contact Form (face or edge)	Material
Enclosure side that is Divider between Propulsion Components and Inside of Chassis		5	edge	AL 7075-T73
Solar Panel Body Al Mount	Solar Panel Deployed Al Mount (hinge)	5mm/35%	face	Al 6061-T6 MIL
Power Management Board	Near Side of Chassis	1.25	edge	Copper strap to enclosure
	Far Side of Chassis	0.2427	edge	Copper strap to enclosure
Power Distribution Board	Near Side of Chassis	1.25	edge	Copper strap to enclosure
	Far Side of Chassis	0.2427	edge	Copper strap to enclosure
Accelerometer	Chassis	12mm	face	Copper strap to enclosure
Sun Sensor	Chassis	28mm	face	Copper strap to enclosure
Radio Cards	Radio Enclosure	5	edge	Al 6061-T6 MIL
Radio Enclosure Sides	Radio Enclosure Front & Back	5	edge	Al 6061-T6 MIL
Radio Enclosure Top & Bottom	Radio Enclosure Sides	5	edge	Al 6061-T6 MIL
Flight Computer Board	Near Side of Chassis	1.25	edge	Copper strap to enclosure
	Far Side of Chassis	0.2427	edge	Copper strap to enclosure
Auxiliary Board	Near Side of Chassis	1.25	edge	Copper strap to enclosure
	Far Side of Chassis	0.2427	edge	Copper strap to enclosure
Extra Interfaces Board	Near Side of Chassis	1.25	edge	Copper strap to enclosure
	Far Side of Chassis	0.2427	edge	Copper strap to enclosure
Cathode	Mount	2.34mm	face	Alumina
Tank Shell Sides	Tank Shell Top and Bottom	5	edge	Titanium
Fuel Lines	Thruster	14mm	face	Alumina
	Cathode	14mm	face	Alumina

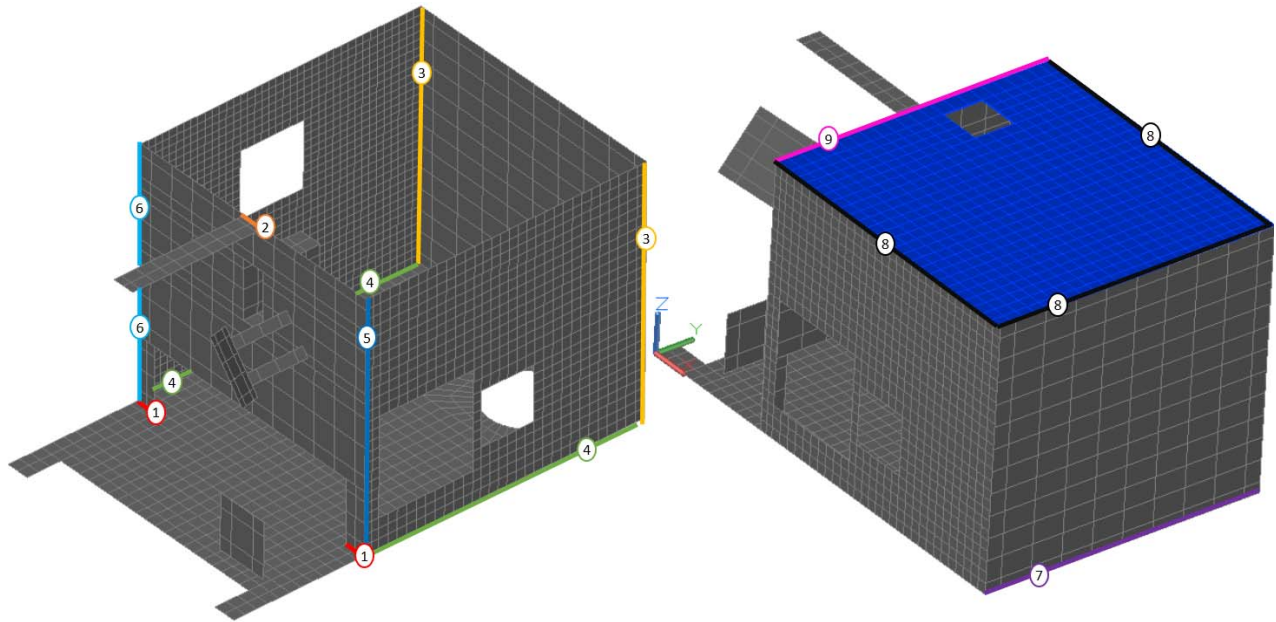


Figure 9. Contacts Calculated from Bolt Assumptions Locations

Table 13. TD Model Contacts Calculated from Bolt Assumptions (see Figure 9 for Contact Number Detail)

Contact Number	Number of Bolts	Conduction Coefficient [W/C]	Contact Form (face of edge)	Tolerance [mm]
1	0	0	edge	1
2	2	6.334	edge	1
3	18	57.005	edge	1
4	12	38.003	edge	1
5	9	28.502	edge	10
6	9	28.502	edge	1
7	7	22.168	edge	1
8	15	47.504	edge	1
9	8	25.335	edge	1
Cathode Mount to Enclosure	2	6.334	edge	1
Camera Mount to Enclosure	2	6.334	edge	1

E. DAC1 Specific Heater Locations

Figure 10 and Figure 11 show the location of heater controllers. The red lines indicate the nodes that have power applied. For all heaters the sensor location is the coldest node included in the heated location.

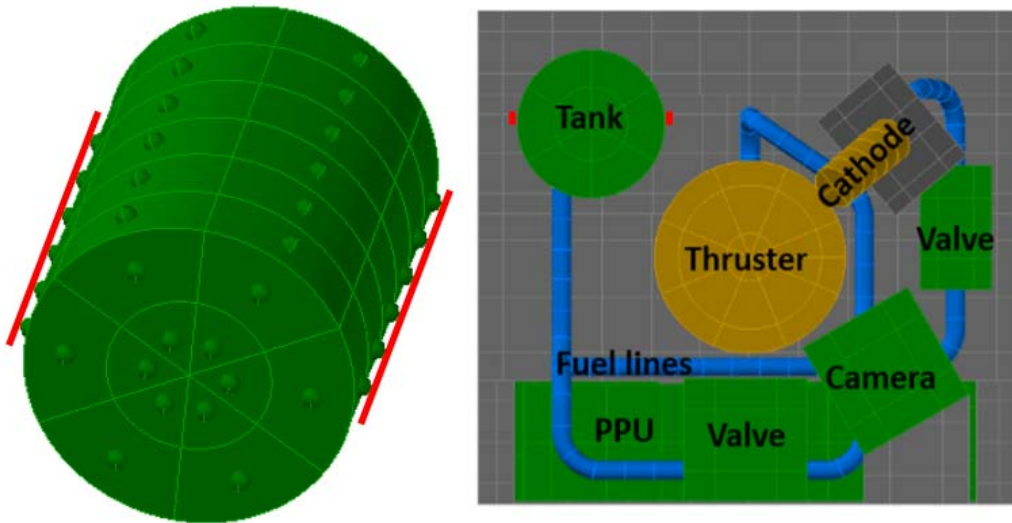


Figure 10. Tank Heater Location Shown in Red

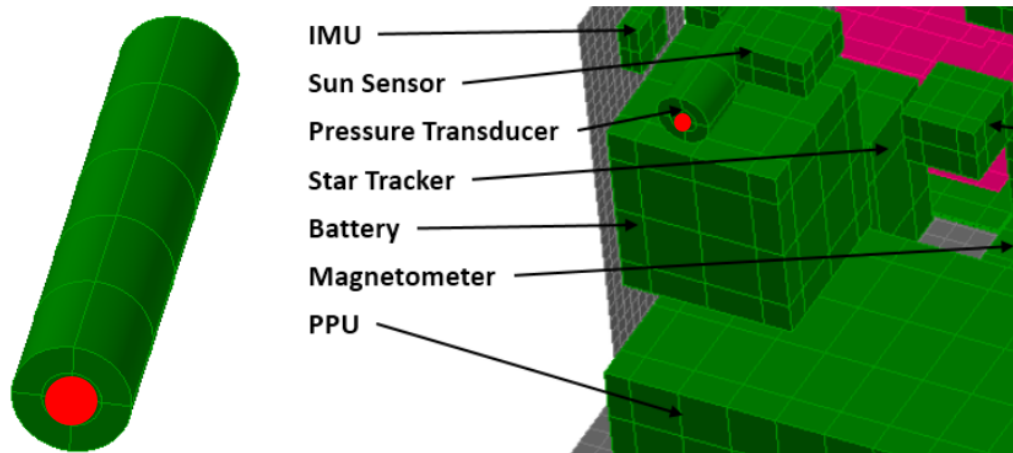


Figure 11. Pressure Transducer Heater Location Shown in Red

Figure 12 shows the location of the power applied to the thruster cylinder. The nodes indicated by the red circle represent the thruster anode and are the nodes to which the power is applied.

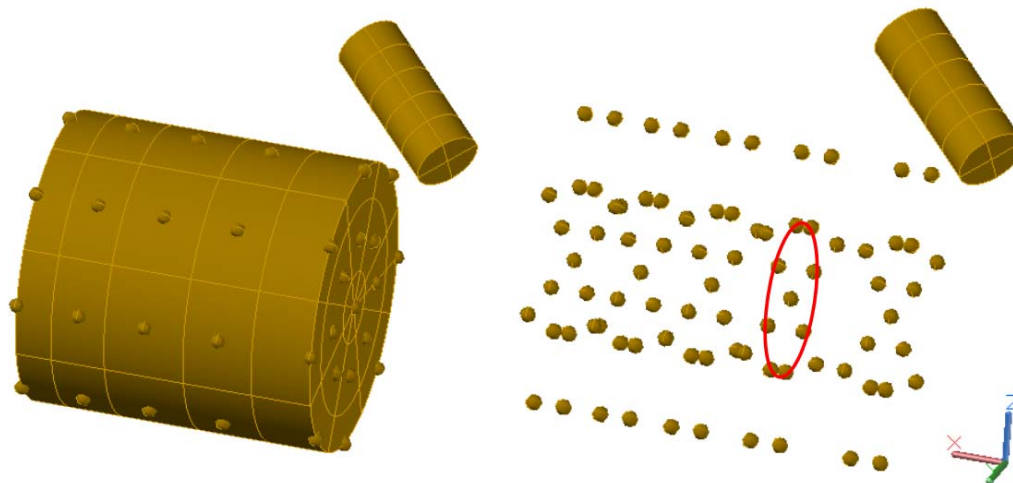


Figure 12. Thruster Location of Power Applied